Syntheses and Structural Characterizations of Ferra- and Cobaltacarborane Complexes Derived from the *arachno*-6-R-5,6,7-$C_3B_7H_{12}$ [R- = $NCCH_2$-, $MeOC(O)CH_2$-, $MeC(O)CH_2$-] Tricarbaborane[1]

Beverly A. Barnum, Patrick J. Carroll, and Larry G. Sneddon*

Department of Chemistry, University of Pennsylvania, Philadelphia, Pennsylvania 19104-6323

Received October 18, 1996[⊗]

A series of ferratricarbaboranyl complexes, *closo*-1-(η-C_5H_5)$FeRC_3B_7H_9$ [R- = H-, $NCCH_2$-, $MeOC(O)CH_2$-], have been generated by the reactions of (η-C_5H_5)$Fe(CO)_2I$ with tricarbaboranyl *arachno*-6-R-5,6,7-$C_3B_7H_{11}^-$ anions. Structural characterizations of *closo*-1-(η-C_5H_5)Fe-2-($NCCH_2$)-2,3,4-$C_3B_7H_9$, **1c**, *closo*-1-(η-C_5H_5)Fe-3-($NCCH_2$)-2,3,4-$C_3B_7H_9$, **1d**, *closo*-1-(η-C_5H_5)Fe-2-($MeCH_3OC(O)CH_2$)-2,3,4-$C_3B_7H_9$, **2b**, and *closo*-1-(η-C_5H_5)-Fe-3-($MeOC(O)CH_2$)-2,3,4-$C_3B_7H_9$, **2c**, show the ferratricarbaboranyl cages in these complexes have closo-octadecahedral structures containing carbon atoms in the two four-coordinate positions closest to the iron. Other isolated products arise from further reactions of the side chain groups, with crystallographically characterized products including the multicage complex ($\mu_{2,12'}$-CH_2)[*closo*-1-(η-C_5H_5)Fe-2,3,4-$C_3B_7H_9$][*arachno*-5′-($NCCH_2$)-5′,7′,9′,12′,11′-$C_4NB_7H_{10}$], **1e**, and the first polyboron metalla*pentacarba*borane *nido*-2-(η-C_5H_5)Fe-7-Me-7,8,9,-10,12-$C_5B_6H_{10}$, **3c**. Cobaltatricarbaboranes of general formula 1-(η-C_5H_5)$Co(NCCH_2)C_3B_7H_9$, **4b**−**d**, along with the unique multimetal cluster *commo*-*Co*-[*closo*-1-Co-8,9-((η-C_5H_5)$Co)_2$-2,3,5-$C_3B_7H_{10}$][*closo*-2′-Co-3′-($NCCH_2$-CH_2)-1′,10′-$C_2B_7H_8$], **4e**, were isolated from the reaction of cobalt chloride with a mixture of the *arachno*-6-$NCCH_2$-5,6,7-$C_3B_7H_{11}^-$ and cyclopentadienyl anions.

Introduction

We recently reported studies of the coordination properties of the monoanion derived from the *nido*-6-Me-5,6,9-$C_3B_7H_{10}$ tricarbadecaborane[2] (Figure 1a) that demonstrated it can bind strongly to transition metals and function as either an η^6 5-electron or an η^4 3-electron ligand, analogous to η^5-$C_5H_5^-$ or η^3-$C_3H_5^-$, respectively.[3,4] In this paper, we describe the first investigations of the metal coordination chemistry of the related 10-vertex *arachno*-tricarbaboranes *arachno*-6-R-5,6,7-$C_3B_7H_{12}$ [R- = $NCCH_2$-, $MeC(O)CH_2$-, $MeOC(O)CH_2$-][5] (Figure 1b). As discussed below, these studies have resulted in a wide range of new metallacarborane complexes, including the first polyboron metalla*pentacarba*borane complex, that illustrate the unusual reactivity of the *arachno*-6-R-5,6,7-$C_3B_7H_{11}^{1-}$ anions.

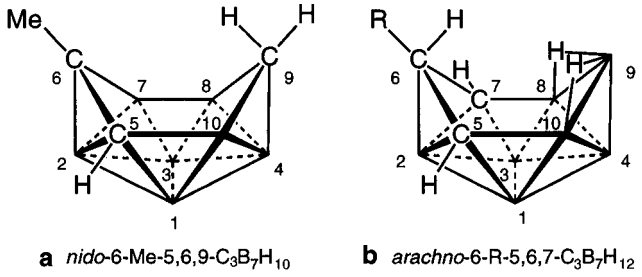

Figure 1. Structures and numbering schemes of the (a) *nido*-6-Me-5,6,9-$C_3B_7H_{10}$ and (b) *arachno*-6-R-5,6,7-$C_3B_7H_{12}$ tricarbaboranes.

Experimental Section

General Procedures and Materials. Unless otherwise noted, all reactions and manipulations were performed in dry glassware under a nitrogen atmosphere using inert-atmosphere techniques as described by Shriver.[6] The *arachno*-6-($NCCH_2$)-5,6,7-$C_3B_7H_{12}$, *arachno*-6-($MeC(O)CH_2$)-5,6,7-$C_3B_7H_{12}$, and *arachno*-6-($MeOC(O)CH_2$)-5,6,7-$C_3B_7H_{12}$ tricarbaboranes were prepared as previously reported.[5] (η-C_5H_5)$Fe(CO)_2I$ was purchased from Strem or Aldrich and used as received. $CoCl_2$ was dried for 15 h at 120 °C *in vacuo* and stored under a nitrogen atmosphere until used. Solvents were distilled from appropriate drying agents under nitrogen before use.

^{11}B NMR spectra at 160.5 or 64.2 MHz, ^{13}C NMR spectra at 125.7 or 50.3 MHz, and ^1H NMR spectra at 500.1 or 200.1 MHz were obtained on Bruker AM-500 and AC-200 spectrometers equipped with the appropriate decoupling accessories. All ^{11}B chemical shifts are referenced to external $BF_3{\cdot}OEt_2$ (0.0 ppm), with a negative sign indicating an upfield shift. Proton and carbon chemical shifts were measured relative to internal residual-protons or carbons from the lock solvent and are referenced to TMS (0.0 ppm). NMR data are presented in Table 1.

High- and low-resolution mass spectra were obtained on a VG-ZAB-E high-resolution mass spectrometer and are reported as *m/z* values. Infrared spectra were obtained on a Perkin-Elmer 1430 spectrophotometer and are listed in the Supporting Information. Preparative thin-layer chromatography was conducted on 0.5 mm (20 × 20 cm) silica gel F-254 plates (Merck 5744). Measurements of the effective magnetic moments of paramagnetic complexes were accomplished by the Evans method[7] using a 2 mm coaxial insert.

[⊗] Abstract published in *Advance ACS Abstracts,* March 1, 1997.

(1) Dedicated to Professor Dr. Walter Siebert on the occasion of his 60th birthday.

(2) Kang, S. O.; Furst, G. T.; Sneddon, L. G. *Inorg. Chem.* **1989**, *28*, 2339−2347.

(3) (a) Plumb, C. A.; Carroll, P. J.; Sneddon, L. G. *Organometallics* **1992**, *11*, 1665−1671. (b) Plumb, C. A.; Carroll, P. J.; Sneddon, L. G. *Organometallics* **1992**, *11*, 1672−1680. (c) Plumb, C. A.; Sneddon, L. G. *Organometallics* **1992**, *11*, 1681−1685.

(4) (a) Weinmann, W.; Wolf, A.; Pritzkow, H.; Siebert, W.; Barnum, B. A.; Carroll, P. J.; Sneddon, L. G. *Organometallics* **1995**, *14*, 1911−1919. (b) Barnum, B. A.; Carroll, P. J.; Sneddon, L. G. *Organometallics* **1996**, *15*, 645−654.

(5) (a) Su, K.; Barnum, B. A.; Carroll, P. J.; Sneddon, L. G. *J. Am. Chem. Soc.* **1992**, *114*, 2730−2731. (b) Su, K.; Carroll, P. J.; Sneddon, L. G. *J. Am. Chem. Soc.* **1993**, *115*, 10004−100017.

(6) Shriver, D. F.; Drezdzon, M. A. *Manipulation of Air Sensitive Compounds*, 2nd ed.; Wiley: New York, 1986.

S0020-1669(96)01253-0 CCC: $14.00

Table 1. NMR Data

no.	compound[a]	nucleus	δ, ppm (multiplicity, assignment, J (Hz))
1a	*closo*-1-CpFe-2,3,4-$C_3B_7H_{10}$	^{11}B[b]	3.4 (d, B9, 153); −4.7 (d, B8, 170); −10.9 (d, B5,B7, 147); −26.1 (d, B10, 162); −28.9 (d, B11, 167); −32.5 (d, B6, 158)
		$^{1}H\{^{11}B\}$[d]	6.86 (s, 1H, CH); 6.24 (s, 1H, CH); 4.76 (s, 5H, Cp); 2.82 (s, 1H, BH); 2.70 (s, 1H, BH); 2.23 (s, 1H, BH); 1.56 (s, 1H, BH); 1.38 (s, 1H, CH); 0.42 (s, 1H, BH); 0.34 (s, 1H, BH); 0.17 (s, 1H, BH)
		2D $^{11}B-^{11}B$[c]	B9−B7;[g] B9−B11; B9−B10; B9−B6; B8−B5;[g] B8−B11; B8−B10; B5−B11;[g] B5−B6;[g] B7−B10;[g] B11−B10; B11−B6
1b	*closo*-1-CpFe-4-($NCCH_2$)-2,3,4-$C_3B_7H_9$	^{11}B[c]	3.9 (d, B9, 157); −2.0 (d, B8, 153); −9.3 (d, B5,B6, *f*); −24.7 (d, B11,B10, 169); −32.6 (d, B7, 159)
		$^{1}H\{^{11}B\}$[d]	7.68 (br s, 1H, CH); 7.56 (br s, 1H, CH); 6.26 (s, 1H, BH); 4.90 (s, 5H, Cp); 4.18 (d of m, 2H, CH_2); 2.87 (s, 1H, BH); 2.79 (s, 1H, BH); 2.55 (s, 1H, BH); 1.53 (s, 1H, BH)
1c	*closo*-1-CpFe-2-($NCCH_2$)-2,3,4-$C_3B_7H_9$	^{11}B[c]	5.4 (d, B9, 161); 2.4 (d, B8, 168); −6.4 (d, B5, 150); −8.9 (d, B6, 156); −22.9 (d, B11, 172); −26.0 (d, B10, 179); −30.7 (d, B7, 159)
		$^{1}H\{^{11}B\}$[d]	7.09 (s, 1H, C3−H); 4.88 (s, 5H, Cp); 4.48 (d of d, 2H, CH_2, 19, 12); 2.86 (s, 1H, BH); 2.71 (s, 1H, BH); 2.37 (s, 1H, BH); 1.63 (s, 1H, BH); 0.92 (br s, 1H, C4−H); 0.58 (s, 1H, BH); 0.28 (s, 1H, BH)
1d	*closo*-1-CpFe-3-($NCCH_2$)-2,3,4-$C_3B_7H_9$	^{11}B[c]	7.8 (d, B9, 156); −5.8 (d, B8, 174); −10.3 (d, B5,B6, ∼145[f]); −26.1 (d, B11, 160); −28.7 (d, B10, 167); −31.2 (d, B7, 158)
		$^{1}H\{^{11}B\}$[d]	6.39 (s, 1H, CH); 4.87 (s, 5H, Cp); 4.44 (s, 2H, CH_2); 2.93 (s, 1H, BH); 2.69 (s, 1H, BH); 2.31 (s, 1H, BH); 1.73 (s, 1H, BH); 1.43 (s, 1H, CH); 0.57 (s, 1H, BH)
1e	($\mu_{2,12'}$-CH_2)(*closo*-1-CpFe-2,3,4-$C_3B_7H_9$)-[*arachno*-5′-($NCCH_2$)-5′,7′,9′,12′,11′-$C_4NB_7H_{10}$]	^{11}B[c]	9.8 (d, 1B); 3.3 (d, 3B); −1.1 (d, 1B); −2.9 (d, 1B); −9.9 (d, 2B); −17.4 (d, 1B); −21.4 (d, 1B); −23.4 (d, 1B); −25.3 (d, 1B); −28.7 (d, 1B); −32.4 (d, 1B)
		$^{1}H\{^{11}B\}$[d]	7.64 (d of m); 7.08 (s, CH); 4.81 (s, Cp); 3.50 (br s, BH), 3.45 (d, CH); 3.41 (s, BH); 3.06 (d, CH); 2.75 (s, BH); 2.52 (s, CH); 2.40 (d, CH); 0.92 (br m, CH); 0.52 (s, BH); 0.37 (s, BH); 0.23 (s, BH)
1f		^{11}B[c]	−1.5 (d, 166); −4.5 (d, *f*); −9.5 (d, 161); −14.8 (d, 143); −23.9 (d, 128); −28.2 (d, 174); −33.3 (d, 141); −37.2 (d, *f*); −51.9 (d, 163)
		$^{1}H\{^{11}B\}$[d]	6.28 (br s, CH); 4.84 (s, Cp); 4.80 (d of d, CH_2, 6, 20); 4.47 (s); 3.42 (s, BH); 2.91 (s); 2.69 (s, BH); 2.81 (s); 2.52 (br s); 2.28 (br d); 2.11 (s, BH); 1.93 (s, BH); 1.62 (br s); 1.38 (s, BH); 0.86 (t); 0.55 (s, BH); 0.24 (s, BH); −3.14 (s, μ-BH)
1g		^{11}B[b]	9.5 (d, 1B, *f*); 5.5 (d, 1B, *f*); 3.4 (d, 1B, *f*); 1.7 (d, 1B, *f*); −1.4 (d, 1B, *f*); −4.9 (d, 1B, 170); −10.4 (d, 2B, *f*); −17.5 (d, 1B, *f*); −21.9 (d, 1B, 136); −23.7 (d, 1B, 140); −26.0 (d, 1B, 149); −28.8 (d, 1B, 179); −31.0 (d, 1B, 145)
		$^{1}H\{^{11}B\}$[d]	7.62 (d of m); 6.35 (s, CH); 5.03 (s); 4.78 (s, Cp); 4.19 (d of m); 3.50 (s, BH); 3.13 (s, CH); 3.00 (s, BH); 2.95 (d, CH); 2.88 (s, BH); 2.82 (s, BH); 2.71 (s, BH); 2.46 (s, CH); 2.30 (s, BH); 1.56 (s, BH); 1.33 (s, CH); 0.92 (s, CH); 0.50 (s, BH); 0.22 (s, BH)
2b	*closo*-1-CpFe-2-($MeOC(O)CH_2$)-2,3,4-$C_3B_7H_9$	^{11}B[c]	4.9 (d, B9, 163); 1.8 (d, B8, 173); −6.2 (d, B5, 173); −9.3 (d, B6, 167); −23.3 (d, B11, 163); −26.2 (d, B10, 156); −30.6 (d, B7, 156)
		$^{1}H\{^{11}B\}$[d]	6.92 (s, 1H, C3−H); 4.79 (s, 5H, Cp); 4.38 (d of d, CH_2, 35, 15); 3.84 (s, CH_3); 2.79 (s, 1H, BH); 2.60 (s, 1H, BH); 2.25 (s, 1H, BH); 1.69 (s, CH); 0.85 (m, 1H, C5-H); 0.45 (s, 1H, BH); 0.31 (s, 1H, BH); 0.21 (s, 1H, BH)
2c	*closo*-1-CpFe-3-($MeOC(O)CH_2$)-2,3,4-$C_3B_7H_9$	^{11}B[c]	7.3 (d, B9, 157); −6.2 (d, B8, *f*); −10.0 (d, B5, *f*); −11.0 (d, B6, ∼140[f]); −26.3 (d, B11, 155); −29.0 (d, B10, 154); −31.1 (d, B7, 154)
		$^{1}H\{^{11}B\}$[d]	6.24 (s, 1H, CH); 4.86 (s, 5H, Cp); 4.40 (d of d, 2H, CH_2); 3.78 (s, 3H, CH_3); 2.85 (s, 1H, BH); 2.64 (s, 1H, BH); 2.19 (s, 1H, BH); 1.51 (s, 1H, BH); 0.88 (s, 1H, CH); 0.42 (s, 1H, BH); 0.33 (s, 1H, BH); 0.18 (s, 1H, BH)
		2D $^{11}B-^{11}B$[c]	B9−B10; B9−B11; B9−B7; B8−B5; B8−B10; B8−B11; B5−B6; B5−B11; B6−B11; B10−B11; B10−B7; B9−B6 missing
3b	*commo-Fe*-(*closo*-1-Fe-2,3,4-$C_3B_7H_{10}$)-(*closo*-1′-Fe-2′,3′,5′-$C_3B_7H_{10}$)	^{11}B[c]	8.2 (d, 2B); −3.6 (d, 4B); −5.2 (d, 2B); −21.9 (d, 3B); −22.2 (d, 1B); −29.3 (d, 1B); −31.3 (d, 1B)
		$^{1}H\{^{11}B\}$[d]	7.60 (s, CH); 6.57 (s, CH); 3.68 (s, CH); 3.15 (s, BH); 3.07 (s, BH); 2.76 (s, 2BH); 2.41 (s, 2CH); 1.82 (s, CH); 0.86 (s, BH); 0.56 (s, 2BH)
3c	*nido*-2-CpFe-7-Me-7,8,9,10,12-$C_5B_6H_{10}$	^{11}B[b]	9.5 (d, B6, 135); −1.6 (d, B3, 153); −10.1 (d, B4, 161); −18.4 (d, B11, 145); −21.8 (d, B5, 144); −33.8 (d, B1, 143)
		$^{1}H\{^{11}B\}$[d]	4.52 (s, 5H, Cp); 3.65 (s, 1H, BH); 3.04 (s, 1H, BH); 2.76 (s, 3H, CH_3); 2.66 (br, 1H, CH); 2.12 (br s, 1H, CH); 1.57 (s, 1H, BH); 1.38 (s, 1H, BH); 1.16 (s, 2H, BH); 1.07 (br s, 1H, CH); 0.85 (br s, 1H, CH);
		$^{13}C\{^{1}H\}$[e]	94.8 (C7); 80.4 (Cp); 38.9 (cage *C*H); 34.6 (cage *C*H); 29.5 (cage *C*H); 28.9 (cage *C*H); 18.0 (CH_3)
		2D $^{11}B-^{11}B$[c]	B1−B3; B1−B4; B1−B5; B1−B6; B3−B4 (wk); B4−B5; B5−B6; B5−B11; B6−B11 (wk)

[a] In CD_2Cl_2. [b] 160.4 MHz. [c] 64.2 MHz. [d] 200.1 MHz. [e] 50.3 MHz. [f] Could not be determined due to overlapping resonances. [g] B5−B7 coincidental resonances.

Reaction of (η-C_5H_5)Fe(CO)$_2$I with *arachno*-6-(NCCH$_2$)-5,6,7-$C_3B_7H_{11}^-$. A solution of K[6-(NCCH$_2$)-5,6,7-$C_3B_7H_{11}$], prepared from the reaction of 6-(NCCH$_2$)-5,6,7-$C_3B_7H_{12}$ (0.40 g, 2.4 mmol) with KH (0.09 g, 3.9 mmol) in THF (10 mL), was added dropwise to a stirred solution of CpFe(CO)$_2$I (0.73 g, 2.4 mmol) in THF (20 mL). After 14 h at room temperature, the solvent was vacuum-evaporated. The oily green residue was dissolved in CH_2Cl_2, the solution was filtered, and the filtrate was chromatographed (silica gel/CH_2Cl_2) to give seven fractions. **1a**, *closo*-1-(η-C_5H_5)Fe-2,3,4-$C_3B_7H_{10}$: green-blue (R_f 0.95); 0.026 g, 0.11 mmol, 4.5%; HRMS calcd for $^{12}C_8{}^1H_{15}{}^{11}B_7{}^{56}Fe$ 244.1175, found 244.1177; mp 153 °C. **1b**, *closo*-1-(η-C_5H_5)Fe-4-(NCCH$_2$)-2,3,4-$C_3B_7H_9$: green-blue (R_f 0.74); 0.022 g, 0.08 mmol, 3.3%; HRMS calcd for $^{12}C_{10}{}^1H_{16}{}^{11}B_7{}^{56}Fe^{14}N$ 283.1284, found 283.1289; mp 131 °C. **1c**, *closo*-1-(η-C_5H_5)Fe-2-(NCCH$_2$)-2,3,4-$C_3B_7H_9$: blue (R_f 0.72); 0.032 g, 0.11 mmol, 4.7%; HRMS calcd for $^{12}C_{10}{}^1H_{16}{}^{11}B_7{}^{56}Fe^{14}N$ 283.1284, found 283.1290; mp 125 °C. **1d**, *closo*-1-(η-C_5H_5)Fe-3-(NCCH$_2$)-2,3,4-$C_3B_7H_9$: blue-purple (R_f 0.64); 0.100 g, 0.36 mmol, 14.8%; HRMS calcd for $^{12}C_{10}{}^1H_{16}{}^{11}B_7{}^{56}Fe^{14}N$ 283.1284, found 283.1292; mp 107 °C. **1e**, ($\mu_{2,12'}$-CH$_2$)[*closo*-1-(η-C_5H_5)Fe-2,3,4-$C_3B_7H_9$][*arachno*-5′-(NCCH$_2$)-5′,7′,9′,12′,11′-$C_4NB_7H_{10}$]: blue (R_f 0.41); 0.050 g, 0.11 mmol, 4.7%; HRMS calcd for $^{12}C_{15}{}^1H_{28}{}^{11}B_{14}{}^{56}Fe^{14}N_2$: 446.2904, found 446.2932; mp 162 °C. **1f**, [(η-C_5H_5)Fe(NCCH$_2$)$C_3B_7H_9$](NCCH$_2$-$C_3B_7H_{10}$): green-blue (R_f 0.54); 0.165 g, 0.37 mmol, 15.5%; HRMS calcd for $^{12}C_{15}{}^1H_{28}{}^{11}B_{14}{}^{56}Fe^{14}N_2$ 446.2904, found 446.2923; mp 161 °C. **1g**, [(η-C_5H_5)Fe(NCCH$_2$)$C_3B_7H_9$](NCCH$_2C_3B_7H_{10}$): blue (R_f 0.49); 0.060 g, 0.14 mmol, 5.6%; HRMS calcd for $^{12}C_{15}{}^1H_{28}{}^{11}B_{14}{}^{56}Fe^{14}N_2$ 446.2904, found 446.2920; mp 86 °C.

Reaction of (η-C_5H_5)Fe(CO)$_2$I with *arachno*-6-(MeOC(O)CH$_2$)-5,6,7-$C_3B_7H_{11}^-$. A solution of K[6-(MeOC(O)CH$_2$)-5,6,7-$C_3B_7H_{11}$], prepared from the reaction of 6-(MeOC(O)CH$_2$)-5,6,7-$C_3B_7H_{12}$ (0.05 g, 0.23 mmol) with KH (0.01 g, 0.4 mmol) in THF (5 mL), was added dropwise to a stirring solution of CpFe(CO)$_2$I (0.07 g, 0.23 mmol) in THF (10 mL). After 14 h at room temperature, the solvent was vacuum-evaporated. The oily blue residue was dissolved in CH_2Cl_2, the solution was filtered, and the filtrate was chromatographed (silica gel/benzene) to give three fractions. **1a**, *closo*-1-(η-C_5H_5)Fe-2,3,4-$C_3B_7H_{10}$: blue (R_f 0.93); 0.015 g, 0.06 mmol, 26.9%; vide infra. **2b**, *closo*-1-(η-C_5H_5)Fe-2-(MeOC(O)CH$_2$)-2,3,4-$C_3B_7H_9$: blue (R_f 0.71); 0.022 g, 0.07 mmol, 30.4%; HRMS calcd for $^{12}C_{11}{}^1H_{19}{}^{11}B_7{}^{56}Fe^{16}O$ 316.1386, found 316.1388; mp 117 °C. **2c**, *closo*-1-(η-C_5H_5)Fe-3-(MeOC(O)CH$_2$)-2,3,4-$C_3B_7H_9$: deep blue (R_f 0.61); 0.010 g, 0.03 mmol, 13.8%; HRMS calcd for $^{12}C_{11}{}^1H_{19}{}^{11}B_7{}^{56}Fe^{16}O$ 316.1386; found 316.1388; mp 131 °C.

Reaction of (η-C_5H_5)Fe(CO)$_2$I with *arachno*-6-(MeC(O)CH$_2$)-5,6,7-$C_3B_7H_{11}^-$. A solution of K[6-(MeC(O)CH$_2$)-5,6,7-$C_3B_7H_{11}$], prepared from the reaction of 6-(MeC(O)CH$_2$)-5,6,7-$C_3B_7H_{12}$ (0.45 g, 2.48 mmol) with KH (0.15 g, 3.7 mmol) in THF (10 mL), was added dropwise to a stirring solution of CpFe(CO)$_2$I (0.71 g, 2.33 mmol) in THF (20 mL). After 14 h at room temperature, the solvent was vacuum-evaporated. The oily dark green residue was dissolved in CH_2Cl_2, the solution was filtered through a 2 cm plug of cellulose, and the filtrate was chromatographed (silica gel/benzene) to give three fractions. **1a**, *closo*-1-(η-C_5H_5)Fe-2,3,4-$C_3B_7H_{10}$: blue (R_f 0.94); 0.240 g, 1.0 mmol, 42.4%; vide infra. **3b**, *commo-Fe*-(*closo*-1-Fe-2,3,4-$C_3B_7H_{10}$)-(*closo*-1′-Fe-2′,3′,5′-$C_3B_7H_{10}$): red-brown (R_f 0.97); 0.090 g, 0.3 mmol, 12.9%; HRMS calcd for $^{12}C_6{}^1H_{20}{}^{11}B_{14}{}^{56}Fe$ 302.2217, found 302.2206; mp 166 °C dec. **3c**, *nido*-2-(η-C_5H_5)Fe-7-CH$_3$-7,8,9,10,12-$C_5B_6H_{10}$: red (R_f 0.78); 0.085 g, 0.31 mmol, 13.5%; HRMS calcd for $^{12}C_{11}{}^1H_{18}{}^{11}B_6{}^{56}Fe$ 272.1318, found 272.1316; mp 153 °C.

Reaction of Na$^+$C$_5$H$_5^-$, CoCl$_2$, and *arachno*-6-(NCCH$_2$)-5,6,7-$C_3B_7H_{11}^-$. A solution of K[6-(NCCH$_2$)-5,6,7-$C_3B_7H_{11}$], prepared from the reaction of 6-(NCCH$_2$)-5,6,7-$C_3B_7H_{12}$ (0.42 g, 2.57 mmol) with KH (0.15 g, 3.6 mmol) in THF (10 mL), was added dropwise while a solution of Na[C_5H_5] (1.4 mL of 2.0 M solution, 2.8 mmol) in THF (10 mL) was concurrently added dropwise to a stirring solution of $CoCl_2$ (0.37 g, 2.83 mmol) in THF (10 mL), resulting in a color change from bright blue to dark green-brown. After 15 h at room temperature, the solvent was vacuum-evaporated. The oily green residue was dissolved in CH_2Cl_2, the solution was filtered, and the filtrate was chromatographed (silica gel/4:1 CH_2Cl_2−hexane) to give five fractions. **4a**, *closo*-2-(η-C_5H_5)Co-1,6-$C_2B_7H_9$: red (R_f 0.94); 0.039 g, 0.17 mmol, 6.6%; spectroscopic data agree with those previously reported.[8] **4b**, *closo*-1-(η-C_5H_5)Co-3-(NCCH$_2$)-2,3,4-$C_3B_7H_9$: purple (R_f 0.53); 0.035 g, 0.17 mmol, 4.7%; HRMS calcd for $^{12}C_{10}{}^1H_{16}{}^{11}B_7{}^{59}Co^{14}N$ 286.1266, found 286.1383; mp 203 °C. **4c**, *closo*-1-(η-C_5H_5)Co-4-(NCCH$_2$)-2,3,4-$C_3B_7H_9$: orange (R_f 0.36); 0.028 g, 0.10 mmol, 3.9%; HRMS calcd for $^{12}C_{10}{}^1H_{16}{}^{11}B_7{}^{59}Co^{14}N$ 286.1266, found 286.1314; mp 136 °C. **4d**, *closo*-1-(η-C_5H_5)Co-2-(NCCH$_2$)-2,3,4-$C_3B_7H_9$: orange-red (R_f 0.27); 0.032 g, 0.11 mmol, 4.3%; HRMS calcd for $^{12}C_{10}{}^1H_{16}{}^{11}B_7{}^{59}Co^{14}N$ 286.1266, found 286.1345; mp 124 °C; paramagnetic (μ = 1.35). **4e**, *commo-Co*-[*closo*-1-Co-8,9-((η-C_5H_5)Co)$_2$-2,3,5-$C_3B_7H_{10}$][*closo*-2′-Co-3′-(NCCH$_2$CH$_2$)-1′,10′-$C_2B_7H_8$]: peach (R_f 0.15); 0.017 g, 0.03 mmol, 1.1%.

Isomerization Reactions. For all thermolytic studies, ∼5 mg samples were sealed *in vacuo* in 2−3 in. lengths of 5-mm Pyrex tubing and placed in either an oil bath or an insulated, glass-wool-packed quartz tube wrapped in heating tape. Analysis of the reaction was performed by TLC. For **1b**, **1c**, and **1d** no isomerizations were observed when they were heated at 155 °C for 11 h. A 10% conversion of **1c** to **1b** was observed upon heating **1c** for 1 h at 210 °C, with complete conversion found after 1 h at 290 °C. No isomerization of **1d** was observed at any temperature. Conversion of **4d** to **4c**, was found upon heating 1 h at 207 °C, but no change for **4b** was observed under these conditions. Decomposition of **4b**, **4c**, and **4d** was observed upon heating samples at 301°C for 1 h.

Crystallographic Data for 1c, **1d**, **1e**, **2b**, **2c**, **3c, 4a, and 4e.** Single crystals were grown by slow evaporation in air of methylene chloride or pentane solutions.

Collection and Reduction of the Data. X-ray intensity data for **1c**, **1e**, **2b**, **2c**, and **4e** were collected on an Enraf-Nonius CAD4 diffractometer employing graphite-monochromated Mo Kα radiation (λ = 0.710 73 Å) and using the ω−2θ scan technique. The intensity data were corrected for Lorentz and polarization effects, and an empirical absorption correction was applied. X-ray intensity data for **1d**, **3c**, and **4a** were collected on an MSC/RAXIS-IIc area detector employing graphite-monochromated Mo Kα radiation (λ = 0.7107 Å). The intensity data were corrected for Lorentz and polarization effects but not for absorption.

Solution and Refinement of the Structures. X-ray data for **1c**, **1e**, **2b**, **2c,** and **4e** were processed, and the structures were solved by standard heavy-atom Patterson techniques followed by weighted Fourier synthesis. X-ray data were processed, and the structures were solved and refined using the Enraf-Nonius MolEN[9] package on a DEC MicroVAX 3100 computer. Refinement was performed by full-matrix least-squares techniques based on F to minimize the quantity $\sum w(|F_o| - |F_c|)^2$ with $w = 1/\sigma^2(F)$. Non-hydrogen atoms were refined anisotropically. For **1c**, **1e**, and **4e**, hydrogen atoms were not refined. For **2b**, cyclopentadienyl hydrogen atoms were not refined and all other hydrogen atoms were refined isotropically. For **2c**, hydrogen atoms were refined isotropically.

X-ray data for **1d**, **3c,** and **4a** were processed, and the structures were solved and refined using the Molecular Structure Corp. teXsan[10] package on a Silicon Graphics Indigo R4000 computer. The structures for **1d**, **3c,** and **4a** were solved by direct methods (SIR88, SIR92,[11] or SAPI91[12]). Refinement was performed by full-matrix least-squares techniques based on F to minimize the quantity $\sum w(|F_o| - |F_c|)^2$ with $w = 1/\sigma^2(F)$. Non-hydrogen atoms were refined anisotropically. For **1d**, **3c**, and **4a**, cage hydrogens were refined isotropically and all other

(7) (a) Evans, D. F. *J. Chem. Soc.* **1959**, 2003−2005. (b) Carlin, R. L. *J. Chem. Educ.* **1966**, *43*, 521−525. (c) Crawford, T. H.; Swanson, J. *J. Chem. Educ.* **1971**, *48*, 382−386.

(8) (a) Hawthorne, M. F.; George, T. A. *J. Am. Chem. Soc.* **1967**, *89*, 7114−7115. (b) Jones, C. J.; Francis, J. N.; Hawthorne, M. F. *J. Am. Chem. Soc.* **1972**, *94*, 8391−8399. (c) George, T. A.; Hawthorne, M. F. *J. Am. Chem. Soc.* **1969**, *91*, 5475−5482.

(9) *MolEn: An Interactive Structure Solution Procedure*; Enraf-Nonius: Delft, The Netherlands, 1990.

(10) *teXsan*: *Crystal Structure Analysis Package*; Molecular Structure Corp.: The Woodlands, TX, 1985 and 1992.

(11) Burla, M. D.; Camalli, M.; Cascarano, G.; Giacovazzo, C.; Polidori, G.; Spagna, R.; Viterbo, D. *J. Appl. Crystallogr.* **1989**, *72*, 389−393.

(12) Fan H.-F. *R-SAPI88: Structure Analysis Programs with Intelligent Control*; Rigaku Corp.: Tokyo, 1988.

Table 2. Crystallographic Data Collection and Structure Refinement Information for **1c**, **1d**, **1e**, **2b**, **2c**, **3c**, and **4e**

	1c	**1d**	**1e**	**2b**	**2c**	**3c**	**4e**
formula	$C_{10}H_{16}B_7FeN$	$C_{10}H_{16}B_7FeN$	$C_{15}H_{28}B_{14}FeN_2$	$C_{11}H_{19}B_7FeO_2$	$C_{11}H_{19}B_7FeO_2$	$C_{11}H_{18}B_6Fe$	$C_{18}H_{32}B_{14}Co_3N$
fw	281.77	281.77	443.60	314.80	314.80	271.79	590.60
space group	$P2_1/n$	$P2_1/c$	$P\bar{1}$	$P2_1/c$	$P2_1/n$	$P\bar{1}$	$P2_1/c$
Z	4	8	2	4	4	2	4
cell constants							
a, Å	11.086(6)	22.8514(6)	6.703(1)	12.038(2)	8.669(2)	7.7398(6)	15.353(3)
b, Å	8.509(2)	7.8013(2)	13.483(3)	7.889(3)	15.608(2)	12.9563(7)	13.045(5)
c, Å	14.310(5)	16.3808(3)	15.518(3)	16.282(3)	11.554(2)	6.8563(3)	13.513(4)
α, deg			68.82(2)			99.650(4)	
β, deg	97.20(4)	110.719(6)	93.44(1)	103.94(2)	107.36(1)	107.944(4)	109.89(2)
γ, deg			94.25(2)			91.386(2)	
V, Å^3	1339(2)	2731.3(2)	1303.3(6)	1501(1)	1492.2(9)	642.73(7)	2544(1)
μ, cm^{-1}	10.99	10.78	5.83	9.95	10.01	11.39	7.78
crystal size, mm	0.05 × 0.08 × 0.28	0.03 × 0.05 × 0.35	0.075 × 0.20 × 0.325	0.02 × 0.08 × 0.48	0.20 × 0.28 × 0.42	0.50 × 0.30 × 0.050	0.075 × 0.125 × 0.45
D_{calcd}, g cm^{-3}	1.397	1.385	1.130	1.393	1.401	1.404	1.541
radiation (λ, Å)	Mo Kα (0.710 73)	Mo Kα (0.710 73)	Mo Kα (0.710 73)	Mo Kα (0.710 73)	Mo Kα (0.710 73)	Mo Kα (0.710 73)	Mo Kα (0.710 73)
temp, °C	25	25	25	25	25	25	25
θ range, deg	2.0−27.5	2.0−27.5	2.0−27.5	2.0−27.5	2.0−27.5	2.0−25.0	2.0−22.5
h, k, l collected	+14, +11, ±18	±29, ±9, ±20	+8, ±17, ±20	±15, +10, +21	±11, −20, +14	+9, ±1, ±7	+16, ±14, ±14
no. of reflns measd	3434	24 078	6486	3830	3718	5040	3664
no. of unique reflns	3059	5912 (R_{merge} = 0.068)	5973	3447	3419	2031 (R_{merge} = 0.0353)	3494 (R_{merge} = 0.0289)
no. of obsd reflns	1622[a]	3547[a]	2948[a]	1921[a]	2664[a]	1811[a]	2083[a]
no. of params	236	415	299	246	266	215	393
R_1[b]	0.042	0.054	0.049	0.043	0.029	0.033	0.046
R_2[c]	0.045	0.059	0.058	0.050	0.039	0.037	0.047

[a] $F^2 > 3.0\sigma(F^2)$. [b] $R_1 = \sum||F_o| - |F_c||/\sum|F_o|$. [c] $R_2 = (\sum w(|F_o| - |F_c|)^2/\sum w|F_o|^2)^{1/2}$.

Table 3. Selected Bond Distances (Å) and Angles (deg) in **1e**, ($\mu_{2,12'}$-CH_2)[*closo*-1-(η-C_5H_5)Fe-2,3,4-$C_3B_7H_9$][*arachno*-5′-($NCCH_2$)-5′,7′,9′,12′,11′-$C_4NB_7H_{10}$]

Fe1−C2	1.985(4)	C14−C15	1.475(5)	C7′−B8′	1.573(7)
Fe1−C3	1.947(4)	C14−C5′	1.526(6)	C9′−C12′	1.451(5)
Fe1−C4	2.269(5)	C15−N16	1.114(5)	C9′−B4′	1.731(6)
Fe1−B5	2.212(5)	B5−B6	1.844(6)	C9′−B8′	1.723(5)
Fe1−B6	2.212(6)	B5−B8	1.813(8)	C9′−B10′	1.722(7)
Fe1−B7	2.274(5)	B5−B11	1.807(7)	C12′−N11′	1.288(5)
Fe1−C17	2.059(5)	B6−B9	1.807(7)	B1′−B2′	1.732(7)
Fe1−C18	2.045(4)	B6−B11	1.776(9)	B1′−B3′	1.762(7)
Fe1−C19	2.046(5)	B7−B9	1.804(9)	B1′−B4′	1.731(9)
Fe1−C20	2.081(5)	B7−B10	1.800(9)	B1′−B10′	1.776(6)
Fe1−C21	2.087(5)	B8−B10	1.752(6)	B2′−B3′	1.747(8)
C2−C4	1.495(5)	B8−B11	1.712(7)	B2′−B6′	1.865(6)
C2−C13	1.530(5)	B9−B10	1.723(8)	B3′−B4′	1.726(7)
C2−B5	1.572(6)	B9−B11	1.752(7)	B3′−B8′	1.748(8)
C2−B8	1.680(7)	B10−B11	1.810(8)	B4′−B8′	1.769(8)
C3−B6	1.562(7)	C5′−B1′	1.690(6)	B4′−B10′	1.793(6)
C3−B7	1.546(7)	C5′−B2′	1.660(5)	B6′−N11′	1.516(6)
C3−B9	1.629(8)	C5′−B6′	1.729(6)	C17−C18	1.397(6)
C4−B7	1.738(6)	C5′−B10′	1.569(7)	C17−C21	1.409(6)
C4−B8	1.765(7)	C7′−B2′	1.648(8)	C18−C19	1.404(7)
C4−B10	1.697(7)	C7′−B3′	1.663(7)	C19−C20	1.403(5)
C13−C12′	1.503(6)	C7′−B6′	1.709(6)	C20−C21	1.386(7)

C13−C2−B8	117.7(3)	B6−C3−B7	112.9(4)
C2−C4−B7	123.0(4)	C2−B5−B6	116.3(3)
C3−B6−B5	116.1(4)	C3−B7−C4	115.5(3)
B6′−C5′−B10′	108.0(4)	C14−C5′−B6′	119.1(3)
C14−C5′−B10′	120.4(3)	B6′−C7′−B8′	109.5(3)
C12′−C9′−B8′	102.5(3)	C12′−C9′−B10′	104.3(3)
B8′−C9′−B10′	106.2(3)	C13−C12′−C9′	118.6(4)
C13−C12′−N11′	121.0(3)	C9′−C12′−N11′	120.4(3)
C5′−B6′−C7′	96.7(3)	C7′−B8′−C9′	111.0(3)
C5′−B10′−C9′	112.5(3)	C15−C14−C5′	112.5(4)
C14−C15−N16	178.6(5)		

hydrogen atoms were included as constant contributions to the structure factors and were not refined.

Data collection and refinement details are given in Table 2. Selected bond distances and bond angles are presented in the figure captions and in Tables 3−5. The remaining crystallographic tables may be found in the Supporting Information.

Table 4. Selected Bond Distances (Å) and Angles (deg) in **3c**, *nido*-2-(η^5-C_5H_5)Fe-7-Me-7,8,9,10,12-$C_5B_6H_{10}$

Fe2−C7	1.989(2)	Fe2−C8	2.135(3)	Fe2−C12	2.106(3)
Fe2−C14	2.073(3)	Fe2−C15	2.052(3)	Fe2−C16	2.044(3)
Fe2−C17	2.059(3)	Fe2−C18	2.079(3)	Fe2−B1	2.165(4)
Fe2−B3	2.128(3)	Fe2−B6	2.158(3)	C7−C8	1.441(4)
C7−C12	1.423(4)	C7−C13	1.497(4)	C8−C9	1.543(4)
C8−B3	1.760(4)	C9−B4	1.682(4)	C9−C10	1.525(4)
C9−B3	1.750(4)	C10−B5	1.746(4)	C10−B11	1.571(4)
C10−B4	1.751(4)	C12−B6	1.709(5)	C12−B11	1.645(4)
C15−C16	1.402(6)	C14−C15	1.393(6)	C14−C18	1.363(5)
B1−B3	1.747(5)	C16−C17	1.373(5)	C17−C18	1.366(5)
B1−B6	1.783(5)	B1−B4	1.769(5)	B1−B5	1.784(5)
B5−B6	1.735(5)	B4−B5	1.760(5)	B3−B4	1.745(5)
B6−B11	1.786(4)	B5−B11	1.747(5)		

C8−C7−C13	120.1(3)	C12−C7−C13	122.1(3)
C8−C7−C12	117.2(2)	Fe2−C7−C13	128.2(2)
C7−C8−C9	120.8(2)	C8−C9−C10	115.9(3)
C9−C10−B11	121.3(3)	C10−B11−C12	113.3(3)
C7−C12−B11	117.0(3)		

Results and Discussion

Reaction of $CpFe(CO)_2I$ with *arachno*-6-($NCCH_2$)-5,6,7-$C_3B_7H_{11}^-$. As shown in Figure 1, the *arachno*-6-R-5,6,7-$C_3B_7H_{12}$ tricarbaborane differs from *nido*-6-Me-5,6,9-$C_3B_7H_{10}$ in that it has three adjacent carbons and contains two additional bridge hydrogens. Thus, while the reaction of $CpFe(CO)_2I$ with the *nido*-6-Me-5,6,9-$C_3B_7H_9^-$ anion has been found to yield *closo*-1-CpFe-Me-2,3,4-$C_3B_7H_9$ complexes with two nonadjacent carbons,[3a] the corresponding reaction with the *arachno*-6-R-5,6,7-$C_3B_7H_{11}^-$ anion might be expected to yield *nido*-1-CpFe-2-R-2,4,5-$C_3B_7H_{11}$ complexes, or alternatively, if insertion is accompanied by loss of H_2, adjacent-carbon *closo*-1-CpFe-2-R-2,4,5-$C_3B_7H_9$ complexes. However, all of the ferratricarbaboranyl products produced in the reaction of $CpFe(CO)_2I$ with K[*arachno*-6-($NCCH_2$)-5,6,7-$C_3B_7H_{11}$] were confirmed to have *closo*-1-(η-C_5H_5)Fe-R-2,3,4-$C_3B_7H_9$ cage structures identical to those previously obtained from reactions with the *nido*-6-Me-5,6,9-$C_3B_7H_9^-$ anion. A total of seven metallatricarbaboranes

Table 5. Selected Bond Distances (Å) and Angles (deg) in **4e**, *commo*-*Co*-[*closo*-1-Co-8,9-($(\eta$-$C_5H_5)Co)_2$-2,3,5-$C_3B_7H_{10}$][*closo*-2′-Co-3′-($NCCH_2CH_2$)-1′,10′-$C_2B_7H_8$]

Co1−C1′	1.930(9)	Co1−C2	2.284(9)	Co1−C3	2.066(9)
Co1−C5	2.198(7)	Co1−B3′	2.197(10)	Co1−B4	2.154(10)
Co1−B5′	2.167(10)	Co1−B6	2.102(10)	Co1−B6′	2.140(10)
Co1−B7	2.169(11)	Co1−B9′	2.086(9)	Co8−Co9	2.559(2)
Co8−C2	2.091(8)	Co8−C3	2.038(9)	Co8−C19	2.095(9)
Co8−C20	2.079(10)	Co8−C21	2.054(10)	Co8−C22	2.036(10)
Co8−C23	2.078(10)	Co8−B12	2.061(10)	Co8−B13	2.097(10)
Co9−C5	2.045(8)	Co9−C14	2.038(10)	Co9−C15	2.048(11)
Co9−C16	2.062(13)	Co9−C17	2.073(14)	Co9−C18	2.050(11)
Co9−B4	2.081(10)	Co9−B10	2.029(11)	Co9−B13	2.056(12)
N14′−C13′	1.122(12)	C1′−B3′	1.614(14)	C1′−B4′	1.570(13)
C1′−B5′	1.560(14)	C2−B12	1.704(12)	C2−C3	1.485(13)
C2−B7	1.713(13)	C5−B10	1.689(13)	C5−B4	1.609(13)
C3−B4	1.515(15)	C10′−B7′	1.565(15)	C10′−B8′	1.594(14)
C5−B6	1.684(13)	C12′−C13′	1.431(14)	C11′−C12′	1.520(13)
C10′−B6′	1.593(13)	C15−C16	1.403(23)	C14−C15	1.354(17)
C10′−B9′	1.609(13)	C19−C20	1.395(14)	C16−C17	1.372(24)
C11′−B3′	1.589(13)	C21−C22	1.377(15)	C19−C23	1.393(14)
C14−C18	1.381(17)	B3′−B6′	1.847(15)	C22−C23	1.417(16)
C17−C18	1.335(19)	B4′−B7′	1.785(16)	B3′−B7′	1.820(14)
C20−C21	1.337(13)	B6−B11	1.753(16)	B4′−B8′	1.771(16)
B3′−B4′	1.875(15)	B6′−B9′	1.906(15)	B5′−B8′	1.796(14)
B4′−B5′	1.810(16)	B7−B12	1.806(14)	B6−B7	1.760(15)
B5′−B9′	1.805(15)	B10−B13	1.824(15)	B7−B11	1.751(14)
B6−B10	1.764(14)	B11−B13	1.836(15)	B8′−B9′	1.832(15)
B6′−B7′	1.843(15)	B12−B13	1.822(15)	B10−B11	1.723(17)
B7′−B8′	1.818(16)	B11−B12	1.751(15)		

B3′−Co1−B5′	73.4(4)	C2−Co1−C3	39.5(4)
C2−Co1−B7	45.2(3)	C3−Co1−B4	42.0(4)
C5−Co1−B4	43.4(3)	C5−Co1−B6	46.0(4)
B6−Co1−B7	48.6(4)	Co9−Co8−C3	81.1(3)
Co8−Co9−B4	69.1(4)	C3−C2−B7	119.4(8)
C2−C3−B4	125.7(9)	B4−C5−B6	120.9(7)
C3−B4−C5	118.9(9)	C5−B6−B7	115.1(7)
B3′−C1′−B5′	110.5(8)	C1′−B3′−B6′	109.0(8)
C1′−B3′−C11′	121.3(8)	C11′−B3′−B6′	124.8(8)
C1′−B5′−B9′	110.0(8)	C2−B7−B6	114.4(8)
B3′−B6′−B9′	99.9(7)	B5′−B9′−B6′	102.3(7)
C12′−C11′−B3′	114.8(8)	C11′−C12′−C13′	114.2(9)
N14′−C13′−C12′	178.1(15)		

were produced, of which five could be assigned the structures discussed below on the basis of their spectroscopic and crystallographic data.

$$(\eta\text{-}C_5H_5)Fe(CO)_2I + [\textit{arachno}\text{-}6\text{-}(NCCH_2)\text{-}5,6,7\text{-}C_3B_7H_{11}] \xrightarrow{-2CO,\ -KI,\ -H_2}$$

$$\textit{closo}\text{-}1\text{-}(\eta\text{-}C_5H_5)Fe\text{-}2,3,4\text{-}C_3B_7H_{10} + \textbf{1a}$$

$$\textit{closo}\text{-}1\text{-}(\eta\text{-}C_5H_5)Fe\text{-}4\text{-}(NCCH_2)\text{-}2,3,4\text{-}C_3B_7H_9 + \textbf{1b}$$

$$\textit{closo}\text{-}1\text{-}(\eta\text{-}C_5H_5)Fe\text{-}2\text{-}(NCCH_2)\text{-}2,3,4\text{-}C_3B_7H_9 + \textbf{1c}$$

$$\textit{closo}\text{-}1\text{-}(\eta\text{-}C_5H_5)Fe\text{-}3\text{-}(NCCH_2)\text{-}2,3,4\text{-}C_3B_7H_9 + \textbf{1d}$$

$$(\mu_{2,12'}\text{-}CH_2)[\textit{closo}\text{-}1\text{-}(\eta\text{-}C_5H_5)Fe\text{-}2,3,4\text{-}C_3B_7H_9]\text{-}[\textit{arachno}\text{-}5'\text{-}(NCCH_2)\text{-}5',7',9',12',11'\text{-}C_4NB_7H_{10}] \quad (1)$$

1e

The ^{11}B NMR spectra of *closo*-1-(η-C_5H_5)Fe-2,3,4-$C_3B_7H_{10}$, **1a**, *closo*-1-(η-C_5H_5)Fe-4-($NCCH_2$)-2,3,4-$C_3B_7H_9$, **1b**, *closo*-1-(η-C_5H_5)Fe-2-($NCCH_2$)-2,3,4-$C_3B_7H_9$, **1c**, and *closo*-1-(η-C_5H_5)Fe-3-($NCCH_2$)-2,3,4-$C_3B_7H_9$, **1d**, each contain seven doublet resonances in the range $\delta = +8$ to -33 ppm and are similar to those reported for *closo*-1-(η-C_5H_5)Fe-2-Me-2,3,4-$C_3B_7H_9$ and *closo*-1-(η-C_5H_5)Fe-4-Me-2,3,4-$C_3B_7H_9$.[3a] Likewise, the upfield resonance in the spectrum of each compound is sharp, suggestive of a boron situated between two carbons on the metal-coordinating carborane face. Although these common features indicate that the boron frameworks in all four compounds are similar, the ^{1}H NMR spectra clearly show that the exopolyhedral $-CH_2CN$ groups in **1b**, **1c,** and **1d** are located at different carbon positions in these isomers. Previous ^{1}H NMR studies[3a] of *closo*-1-(η-C_5H_5)Fe-2-Me-2,3,4-$C_3B_7H_9$ and *closo*-1-(η-C_5H_5)Fe-4-Me-2,3,4-$C_3B_7H_9$ have shown that the resonances arising from protons attached the four-coordinate carbons (C2 or C3) closest to the iron appear at low field ($\delta \geq 5.0$ ppm), while those protons bound to one of the five-coordinate carbons (i.e., C4 or C5) appear at higher field ($\delta \leq 1.0$ ppm). Compounds **1a** and **1b** both have two proton shifts at low field ($\delta \approx 6-7$ ppm) consistent with C−H's at positions 2 and 3. Compounds **1a**, **1c**, and **1d**, in addition to having a CH resonance at low field (position 2 or 3), have another C−H at high field ($\delta = \sim 1.5$ ppm) (position 4). For **1c** and **1d**, this is consistent with an exopolyhedral $-CH_2CN$ group bound at one of the four-coordinate C2 or C3 positions.

The above conclusions were confirmed by single-crystal X-ray determinations of **1c**, *closo*-1-(η-C_5H_5)Fe-2-($NCCH_2$)-2,3,4-$C_3B_7H_9$, and **1d**, *closo*-1-(η-C_5H_5)Fe-3-($NCCH_2$)-2,3,4-$C_3B_7H_9$, as shown in the ORTEP drawings in Figures 2 and 3, respectively. As expected, the iron atom in each complex is sandwiched between the cyclopentadienyl and tricarbadecaboranyl ligands. The ferratricarbadecaborane cage fragments in both compounds have gross closo-octadecahedral structures, consistent with their 24-skeletal-electron counts,[13] with the iron

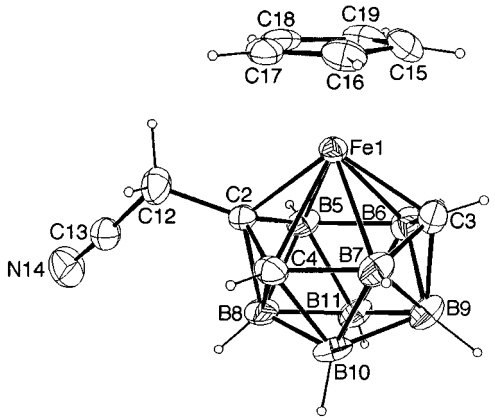

Figure 2. ORTEP drawing of the molecular structure of *closo*-1-(η-C_5H_5)Fe-2-($NCCH_2$)-2,3,4-$C_3B_7H_9$, **1c**. Selected bond lengths (Å): Fe1−C2, 1.965(4); Fe1−C3, 1.952(4); Fe1−C4, 2.242(4); Fe1−B5, 2.232(5); Fe1−B6, 2.238(5); Fe1−B7, 2.254(5); C2−C4, 1.491(6); C2−B5, 1.584(6); C3−B6, 1.560(6); C3−B7, 1.544(7); C4−B7, 1.739(7); B5−B6, 1.847(7); C2−C12, 1.519(6); C12−C13, 1.447(6); C13−N14, 1.126(6). Selected bond angles (deg): C4−C2−B5, 109.4(3); B8−C2−C12, 118.8(3); B6−C3−B7, 113.0(4); C2−C12−C13, 115.8(4); C12−C13−N14, 176.9(5).

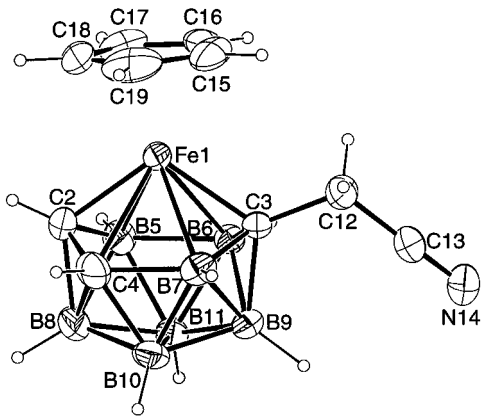

Figure 3. ORTEP diagram of the molecular structure of *closo*-1-(η-C_5H_5)Fe-3-($NCCH_2$)-2,3,4-$C_3B_7H_9$, **1d**. Selected bond lengths (Å): Fe1−C2, 1.938(5); Fe1−C3, 1.974(4); Fe1−C4, 2.228(6); Fe1−B5, 2.250(5); Fe1−B6, 2.255(5); Fe1−B7, 2.256(6); C2−C4, 1.476(8), C2−B5, 1.559(8); C3−B6, 1.577(7); C3−B7, 1.573(7); C4−B7, 1.767(8), B5−B6, 1.822(8), C3−C12, 1.521(6); C12−C13, 1.459(7), N14−C13, 1.137(7). Selected bond angles (deg): C4−C2−B5, 110.7(5); B6−C3−B7, 112.3(4); C12′−C3′−B9′, 119.1(4), C3′−C12′−C13′, 115.1(4); N14′−C13′−C12′, 178.1(6).

atom located in the unique six-coordinate position. Thus, in addition to insertion of the iron atom into the cage, loss of H_2 has occurred from the *arachno*-6-($NCCH_2$)-5,6,7-$C_3B_7H_{11}^-$ anion to produce a formal *nido*-($NCCH_2$)$C_3B_7H_9^-$ ligand. The structural determinations also confirm that the cage carbons have rearranged from their adjacent positions in *arachno*-6-($NCCH_2$)-5,6,7-$C_3B_7H_{12}$ such that two of the cage-carbon atoms now occupy the four-coordinate positions (C2 and C3) closest to the iron atom. It is perhaps surprising that these carbon rearrangements occur under such mild conditions, but the products agree with the established preference of carbon atoms for lower coordinate vertices in carborane clusters.[13c]

(13) (a) Williams, R. E. *Inorg. Chem.* **1971**, *10*, 210−214. (b) Wade, K. *Adv. Inorg. Chem. Radiochem.* **1976**, *18*, 1−66. (c) Williams, R. E. *Adv. Inorg. Chem. Radiochem.* **1976**, *18*, 67−142. (d) Rudolph, R. W. *Acc. Chem. Res.* **1976**, *9*, 446−452. (e) Williams, R. E. In *Electron Deficient Boron and Carbon Clusters*; Olah, G. A., Wade, K., Williams, R. E., Eds.; Wiley: New York, 1991; pp 11−93. (f) Williams, R. E. *Chem. Rev.* **1992**, *92*, 177−207.

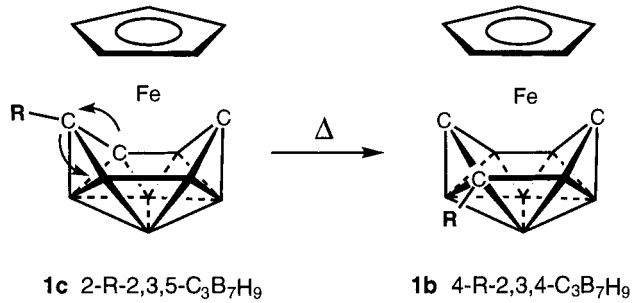

1c 2-R-2,3,5-$C_3B_7H_9$ **1b** 4-R-2,3,4-$C_3B_7H_9$

Figure 4. Possible isomerization process for the conversion of **1c**, *closo*-1-(η-C_5H_5)Fe-2-($NCCH_2$)-2,3,4-$C_3B_7H_9$, to **1b**, *closo*-1-(η-C_5H_5)-Fe-4-($NCCH_2$)-2,3,4-$C_3B_7H_9$.

Bond lengths for both **1c** and **1d** show centered bonding of the Fe atom to the carborane cage and are consistent with those reported for *closo*-1-(η-C_5H_5)Fe-2-Me-2,3,4-$C_3B_7H_9$ and *closo*-1-(η-C_5H_5)Fe-4-Me-2,3,4-$C_3B_7H_9$.[3a] Thus, for **1c**, the Fe distances to C4, B5, B6, and B7 are similar, 2.242(4), 2.232(5), 2.238(5), and 2.254(5) Å, respectively, while the Fe−C2 and −C3 distances are shorter, 1.965(4) and 1.952(4) Å, respectively. Likewise, **1d** shows similar Fe to C4, B5, B6, and B7 bond lengths, 2.228(6), 2.250(5), 2.255(5), and 2.256(6) Å, respectively, and shorter Fe−C2 and Fe−C3 distances, 1.938(5) and 1.974(4) Å. The two compounds are similar in that the $-CH_2CN$ side chains on both compounds are attached to one of the four-coordinate carbons adjacent to the iron, but in **1c**, the side chain is at the carbon (C2) which is adjacent to another carbon (C4) and, in **1d**, it is located at the isolated carbon (C3).

While not crystallographically characterized, the structure of **1b** may be confidently assigned as *closo*-1-(η-C_5H_5)Fe-4-($NCCH_2$)-2,3,4-$C_3B_7H_9$ on the basis of the similarity of its ^{11}B and ^{1}H NMR spectra with those reported for *closo*-1-(η-C_5H_5)-Fe-4-Me-2,3,4-$C_3B_7H_9$.[3a] Further support for this structure comes from the fact that **1c**, *closo*-1-(η-C_5H_5)Fe-2-($NCCH_2$)-2,3,4-$C_3B_7H_9$, quantitatively isomerized to **1b** under similar conditions (1 h at 290 °C) to those observed previously for the isomerization of *closo*-1-(η-C_5H_5)Fe-2-Me-2,3,4-$C_3B_7H_9$ to *closo*-1-(η-C_5H_5)Fe-4-Me-2,3,4-$C_3B_7H_9$.[3a] These rearrangements correspond to a formal "side chain migration" from the C2 to the C4 cage position; however, more detailed NMR studies[3c] of the methyl migrations in the latter compounds using ^{13}C-labeling have proven that the methyl group remains attached to the original cage carbon and the rearrangment from the 2- to the 4-position actually occurs via a skeletal rearrangement of the cage carbons. This cage carbon isomerization probably occurs by a rotation of the C2, C4, B10, B11, B5 pentagonal ring, about B8, as shown in Figure 4.[3c] Compound **1d** was not observed to rearrange at any temperature up to its decomposition, nor was it found as a product of any of the isomerization reactions of **1b** and **1c**. Likewise, no isomers having a carbon arrangement similar to that of **1d** were found in the previous isomerization studies of *closo*-1-(η-C_5H_5)Fe-2-Me-2,3,4-$C_3B_7H_9$ and *closo*-1-(η-C_5H_5)Fe-4-Me-2,3,4-$C_3B_7H_9$.[3c] Thus, it is most likely that **1d** is formed by a carbon rearrangement that occurs during the initial metal insertion reaction.

The production of the parent ferratricarbadecaboranyl compound *closo*-1-(η-C_5H_5)Fe-2,3,4-$C_3B_7H_{10}$, **1a**, in this and the other reactions discussed below, demonstrates that reactions at the side chain, in this case leading to cleavage of the exopolyhedral $-CH_2CN$ group, can be important in these systems. Štíbr *et al.* also recently synthesized this compound by a different route, and the NMR data for **1a** agree with their reported

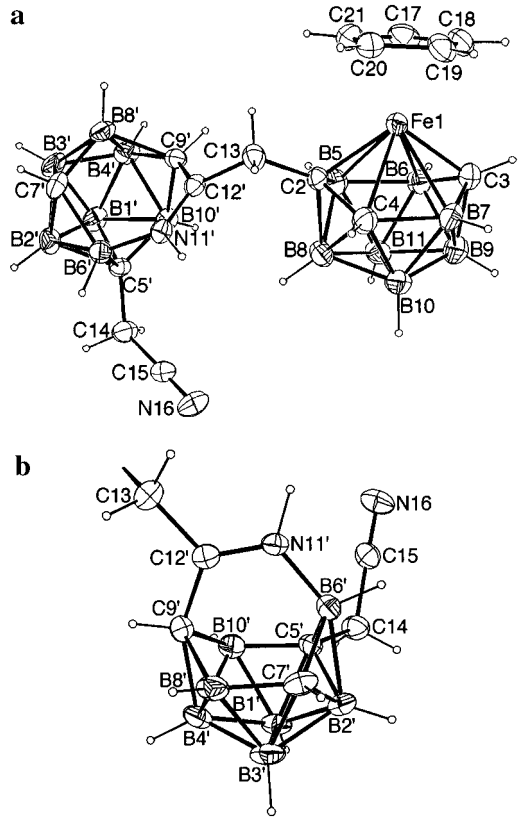

Figure 5. ORTEP diagrams of the molecular structure of **1e**, ($\mu_{2,12'}$-CH_2)[*closo*-1-(η-C_5H_5)Fe-2,3,4-$C_3B_7H_9$][*arachno*-5′-($NCCH_2$)-5′,7′,9′,12′,11′-$C_4NB_7H_{10}$].

values.[14] A 2D $^{11}B-^{11}B$ NMR study (Table 1) also confirms the *closo*-1-(η-C_5H_5)Fe-2,3,4-$C_3B_7H_{10}$ arrangement.

According to their mass spectra, **1e**, **1f**, and **1g** are isomeric compounds of composition $C_{15}H_{28}B_{14}FeN_2$. In agreement with this formula, their ^{11}B NMR spectra each show evidence of 14 boron resonances, and their ^1H NMR spectra each exhibit a single Cp resonance. The structure of **1e**, ($\mu_{2,12'}$-CH_2)[*closo*-1-(η-C_5H_5)Fe-2,3,4-$C_3B_7H_9$][*arachno*-5′-($NCCH_2$)-5′,7′,9′,12′,11′-$C_4NB_7H_{10}$], was established by a single-crystal X-ray determination, as shown in the ORTEP drawings in Figure 5, to be composed of a *closo*-1-(η-C_5H_5)-Fe-2,3,4-$C_3B_7H_9$ fragment linked by a methylene bridge to a 12-vertex azatetracarbaborane cluster, *arachno*-5′-($NCCH_2$)-5′,7′,9′,12′,11′-$C_4NB_7H_{10}$. The structure of the ferratricarbadecaboranyl cage is again based on a closo-octadecahedral geometry and has a skeletal arrangement similar to that determined for **1c** discussed above. An alternate view of the attached azatetracarbaborane cage is shown in Figure 5b, where it can be seen that the carbon (C12′) and nitrogen (N11′) atoms that were part of the nitrile group of the side chain of the ferratricarbadecaboranyl cage have now become inserted into a second tricarbadecaboranyl cage to form a 12-vertex cage fragment of composition $R_2C_4NB_7H_{10}$ (R- = $NCCH_2$- and CH_2- (i.e., methylene bridge)). A cluster of this composition would contain 30 skeletal electrons and thus, on the basis of electron-counting rules,[13] be predicted to adopt a 12-vertex arachno-type ($n + 3$ skeletal electrons) geometry based on a 14-vertex bicapped hexagonal antiprism missing two nonadjacent five-coordinate vertices. The observed stucture is, in fact, consistent with this prediction, containing two puckered six-membered open faces, each containing the C12′ and N11′ atoms. The structure is also consistent with those crystallographically determined for two isoelectronic clusters, the azatricarbaborane *arachno*-7-Me-5,7,14,12-$C_3NB_8H_{11}^-$ and the azamonocarbaborane *arachno*-7-Me-7,12-$CNB_{10}H_{13}^-$.[15]

Alternatively, instead of being considered as part of the cage framework, the C12′ and N11′ atoms in **1e** could be regarded as simply part of an exopolyhedral imine group bridging the tricarbadecaborane cluster, i.e. *arachno*-($\mu_{6',9'}$-RC═NH)-5′-($NCCH_2$)-5′,7′,9′-$C_3B_7H_9$. In this view, the −RC═NH− fragment could then be considered to bond to the arachno-tricarbadecaboranyl fragment by conventional 2-center, 2-electron bonds. The C12′−N11′ bond distance of 1.288(5) Å, which is within the normal range for carbon−nitrogen double bonds, and the bond angles about both C12′ and N11′ (Table 3 and Supporting Information), which suggest sp^2 hybridizations, support this interpretation. These distances and angles are also similar to those found in *arachno*-7-Me-5,7,14,12-$C_3NB_8H_{11}^-$ and *arachno*-7-Me-7,12-$CNB_{10}H_{13}^-$.[15]

Compound **1e** is undoubtedly formed by a process analogous to that involved in the synthesis of *arachno*-7-Me-5,7,14,12-$C_3NB_8H_{11}^-$ and *arachno*-7-Me-7,12-$CNB_{10}H_{13}^-$.[15] The latter compounds are formed in reactions 2 and 3 by a process that is proposed to involve the initial nucleophilic attack of the polyborane anion at the nitrile carbon of acetonitrile, followed by nitrile hydroboration and insertion of the resulting imine into the cage framework.

$$\textit{nido}\text{-}5,6\text{-}C_2B_8H_{11}^- + MeC{\equiv}N \rightarrow \textit{arachno}\text{-}7\text{-}Me\text{-}5,7,14,12\text{-}C_3NB_8H_{11}^- \quad (2)$$

$$\textit{nido}\text{-}5,6\text{-}B_{10}H_{13}^- + MeC{\equiv}N \rightarrow \textit{arachno}\text{-}7\text{-}Me\text{-}7,12\text{-}CNB_{10}H_{13}^- \quad (3)$$

An analogous process leading to the formation of **1e** could involve the initial nucleophilic attack of the *arachno*-6-$NCCH_2$-5,6,7-$C_3B_7H_{11}^-$ anion at the nitrile carbon of the side chain of **1c**, again followed by nitrile hydroboration, imine insertion, carbon skeletal rearrangement, and, finally, protonation (possibly during the workup).

$$\textit{arachno}\text{-}6\text{-}NCCH_2\text{-}5,6,7\text{-}C_3B_7H_{11}^- + N{\equiv}CCH_2R' \xrightarrow{-H_2,\,+H^+} \underset{\textbf{1c}}{} (\mu_{2,12'}\text{-}CH_2)R'[\textit{arachno}\text{-}5'\text{-}(NCCH_2)\text{-}5',7',9',12',11'\text{-}C_4NB_7H_{10}] \quad (4)$$
1e

$$R' = \textit{closo}\text{-}1\text{-}CpFe\text{-}2,3,4\text{-}C_3B_7H_9$$

Due to the similarity of their NMR data, compounds **1f** and **1g** are presumed to have structures related to that of **1e**, but with different arrangements of the carbon atoms in the tricarbadecaboranyl or azatetracarbaborane cage fragments. However, because of the complexity of their NMR spectra, final structural confirmation for these compounds will require X-ray diffraction studies.

Reaction of $CpFe(CO)_2I$ with *arachno*-6-($MeOC(O)CH_2$)-5,6,7-$C_3B_7H_{11}^-$. The reaction of $CpFe(CO)_2I$ and the ester derivative *arachno*-6-($MeOC(O)CH_2$)-5,6,7-$C_3B_7H_{11}^-$ produced, in addition to the parent **1a**, *closo*-1-(η-C_5H_5)Fe-2,3,4-$C_3B_7H_{10}$, which again results from side chain ($MeOC(O)CH_2-$) cleavage, two isomeric complexes of the formula *closo*-1-(η-C_5H_5)Fe-($MeOC(O)CH_2$)$C_3B_7H_9$ (**2b** and **2c**).

(14) Štíbr, B.; Holub, J.; Teixidor, F.; Viñas, C. *Collect. Czech. Chem. Commun.* **1995**, *60*, 2023−2027.

(15) Wille, A. E.; Su, K.; Carroll, P. J.; Sneddon, L. G. *J. Am. Chem. Soc.* **1996**, *118*, 6407−6421.

$$(\eta\text{-}C_5H_5)Fe(CO)_2I + K[\textit{arachno}\text{-}6\text{-}(MeOC(O)CH_2)\text{-}5,6,7\text{-}C_3B_7H_{11}] \xrightarrow{-2CO,\ -KI,\ -H_2} \underset{\textbf{1a}}{\textit{closo}\text{-}1\text{-}(\eta\text{-}C_5H_5)Fe\text{-}2,3,4\text{-}C_3B_7H_{10}} + \underset{\textbf{2b}}{\textit{closo}\text{-}1\text{-}(\eta\text{-}C_5H_5)Fe\text{-}2\text{-}(MeOC(O)CH_2)\text{-}2,3,4\text{-}C_3B_7H_9} + \underset{\textbf{2c}}{\textit{closo}\text{-}1\text{-}(\eta\text{-}C_5H_5)Fe\text{-}3\text{-}(MeOC(O)CH_2)\text{-}2,3,4\text{-}C_3B_7H_9} \quad (5)$$

The structures of *closo*-1-(η-C_5H_5)Fe-2-(MeOC(O)CH_2)-2,3,4-$C_3B_7H_9$, **2b**, and *closo*-1-(η-C_5H_5)Fe-3-(MeOC(O)CH_2)-2,3,4-$C_3B_7H_9$, **2c**, were established by single-crystal X-ray determinations, as shown in the ORTEP drawings in Figures 6 and 7, respectively, and confirm again, that metal insertion into the cage framework was accompanied by loss of H_2 and carbon isomerization to produce complexes containing the formal *nido*-(MeOC(O)CH_2)-2,3,4-$C_3B_7H_9^-$ ligand. Their octadecahedral cage structures, as well as the carbon and side chain locations in **2b** and **2c,** are analogous to those of compounds **1c** and **1d**, respectively. The nature of the side chain appears to have little effect on cage bonding because the cage distances and angles observed for **2b** and **2c**, as well as their NMR data, are very close to those of compounds **1c** and **1d**, respectively.

Reaction of $CpFe(CO)_2I$ with *arachno*-6-(MeC(O)CH_2)-5,6,7-$C_3B_7H_{11}^-$. The reaction with $CpFe(CO)_2I$ and the ketone derivative *arachno*-6-(MeC(O)CH_2)-5,6,7-$C_3B_7H_{11}^-$ produced three metallacarbaboranes.

$$(\eta\text{-}C_5H_5)Fe(CO)_2I + K[\textit{arachno}\text{-}6\text{-}(MeC(O)CH_2)\text{-}5,6,7\text{-}C_3B_7H_{11}] \xrightarrow{-2CO,\ -KI,\ -H_2} \underset{\textbf{1a}}{\textit{closo}\text{-}1\text{-}(\eta\text{-}C_5H_5)Fe\text{-}2,3,4\text{-}C_3B_7H_{10}} + \underset{\textbf{3b}}{\textit{commo-Fe}\text{-}(\textit{closo}\text{-}1\text{-}Fe\text{-}2,3,4\text{-}C_3B_7H_{10})\text{-}(\textit{closo}\text{-}1'\text{-}Fe\text{-}2',3',5'\text{-}C_3B_7H_{10})} + \underset{\textbf{3c}}{\textit{nido}\text{-}2\text{-}(\eta\text{-}C_5H_5)Fe\text{-}7\text{-}Me\text{-}7,8,9,10,12\text{-}C_5B_6H_{10}} \quad (6)$$

Surprisingly, none of the products were the expected substituted complexes, (η-C_5H_5)Fe(MeC(O)CH_2)$C_3B_7H_9$, as observed in reactions discussed above. Two of the products result from side chain cleavage: **1a**, *closo*-1-(η-C_5H_5)Fe-2,3,4-$C_3B_7H_{10}$ (vide infra), and **3b**, *commo-Fe*-(*closo*-1-Fe-2,3,4-$C_3B_7H_{10}$)-(*closo*-1′-Fe-2′,3′,5′-$C_3B_7H_{10}$).[3b] The latter compound is, in fact, the first reported bis(tricarbadecaboranyl)metal complex containing the parent 2,3,4-$C_3B_7H_{10}^-$ ligand.

An exact mass determination on the third product, **3c**, and its ^{11}B NMR spectrum, which showed only six intensity-1 doublets, established that loss of a "BOH" unit from the starting carborane cage had occurred upon formation of the complex. The ^1H NMR spectrum showed, in addition to cyclopentadienyl and methyl resonances, four intensity-1 singlets with line widths and chemical shifts consistent with cage-carbon C−H resonances. These data suggested the incorporation of additional carbon into the original tricarbaborane framework. Such a compound is of great interest since, although such species have been long anticipated, no neutral[16] polyboron carboranes or metallacarboranes with more than four cage carbons were previously reported. A single-crystal X-ray study[17] proved **3c** to be, in fact, the first example of a polyboron metallacarborane complex containing five cage carbon atoms: *nido*-2-(η-C_5H_5)-Fe-7-Me-7,8,9,10,12-$C_5B_6H_{10}$ as shown in the ORTEP drawing in Figure 8.

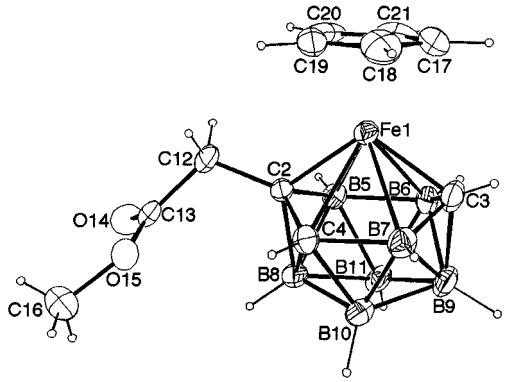

Figure 6. ORTEP diagram of the molecular structure of *closo*-1-(η-C_5H_5)-Fe-2-(MeOC(O)CH_2)-2,3,4-$C_3B_7H_9$, **2b** Selected bond distances (Å): Fe1−C2, 1.959(3); Fe1−C3, 1.946(4); Fe1−C4, 2.248(3); Fe1−B5, 2.209(5); Fe1−B6, 2.228(5); Fe1−B7, 2.267(5); C2−B4, 1.478-(6); C2−B5, 1.578(6), C3−B6, 1.570(7); C3−B7, 1.543(6); C4−B7, 1.762(7); B5−B6, 1.831(7); C2−C12, 1.523(6); C12−C13, 1.503(6); C13−O14, 1.198(6); C13−O15, 1.319(5); O15−C16, 1.426(6). Selected bond angles (deg): C4−C2−B5, 109.2(3); B8−C2−C12, 118.5(3); B6−C3−B7, 113.9(4); C2−C12−C13, 115.1(3); C12−C13−O14, 124.2(4); C12−C13−O15, 111.9(4); O14−C13−O15, 123.9(4); C13−O15−C16, 116.7(4).

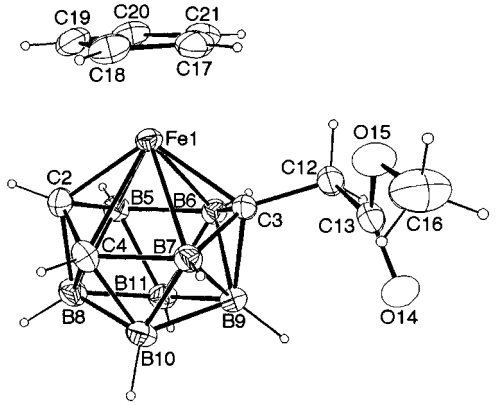

Figure 7. ORTEP diagram of the molecular structure of *closo*-1-(η-C_5H_5)Fe-3-(MeOC(O)CH_2)-2,3,4-$C_3B_7H_9$, **2c**. Selected bond distances (Å): Fe1−C2, 1.951(2); Fe1−C3, 1.981(2); Fe1−C4, 2.259(2); Fe1−B5, 2.237(2); Fe1−B6, 2.235(2); Fe1−B7, 2.271(2); C2−C4, 1.503-(3); C2−B5, 1.563(3); C3−B6, 1.581(3); C3−B7, 1.578(3); C4−B7, 1.754(3); B5−B6, 1.819(3); C3−C12, 1.524(3); C12−C13, 1.508(3); C13−O14, 1.201(2); C13−O15, 1.318(2); C16−O15, 1.448(3). Selected bond angles (deg): C4−C2−B5, 110.6(2); B6−C3−B7, 111.6(2); B9−C3−C12, 116.0(1); C3−C12−C13, 112.8(2); C12−C13−O14, 124.4-(2); C12−C13−O15, 111.8(2); O14−C13−O15, 123.8(2); C13−O15−C16, 115.9(2).

Consistent with its 28-skeletal-electron count,[13] the cage adopts an open nido-type structure, based on a 13-vertex docosahedron missing one six-coordinate vertex, similar to those found for other isoelectronic 12-vertex cage systems, including 2-(η-C_5H_5)Fe-1,7,8,9-$(CH_3)_4C_4B_7H_8$,[18] 2,4-(η-C_5H_5)$_2Co_2$-7,10,-

(16) The monoboron pentacarbon cation, $[1\text{-}RBC_5(CH_3)_5]^+$, has been synthesized and structurally characterized. See: (a) Jutzi, P.; Seufert, A. *J. Organomet. Chem.* **1978**, *161*, C5−C7. (b) Jutzi, P.; Seufert, A.; Buchner, W. *Chem. Ber.* **1979**, *112*, 2488−2493. (c) Dohmeier, C.; Köppe, R.; Robl, C.; Schnöckel, H. J. *J. Organomet. Chem.* **1995**, *487*, 127−130. Monoboron boratabenzene (RBC_5H_5M) complexes are also well-known. See: (d) Herberich, G. E. In *Comprehensive Organometallic Chemistry II;* Abel, E. W., Stone, F. G. A., Wilkinson, G., Eds.; Elsevier: Tarrytown, NY, 1995; pp 197−216 and references therein. (e) Herberich, G. E.; Ohst, H. *Adv. Organomet. Chem.* **1986**, *25*, 199−236 and references therein.

(17) Barnum, B. A.; Carroll, P. J.; Sneddon, L. G. *Organometallics* **1995**, *14*, 4463−4464.

(18) Maxwell, W. M.; Bryan, R. F.; Grimes, R. N. *J. Am. Chem. Soc.* **1977**, *99*, 4008−4015.

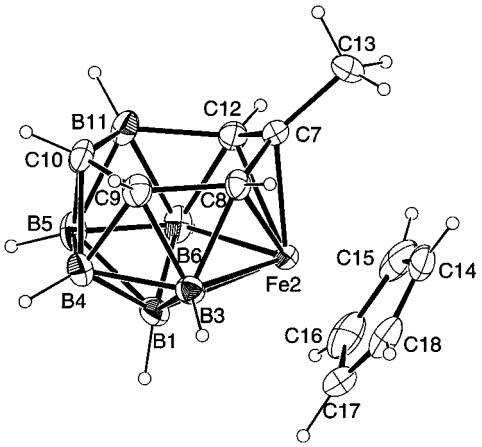

Figure 8. ORTEP diagram of the molecular structure of **3c**, *nido*-2-(η-C_5H_5)Fe-7-Me-7,8,9,10,12-$C_5B_6H_{10}$.

11,12-$C_4B_6H_{10}$,[19] and 2-(η-C_5H_5)Co-7,9,11,12-$(CH_3)_4C_4B_7H_7$.[20] The six-membered open face of the cage contains the five carbon atoms and one boron atom, with all four of the four-coordinate carbon atoms and one boron atom forming a plane. The unique three-coordinate methyl-substituted carbon atom, C7, is distorted out of this plane by 0.46 Å. Given the high carbon content of the cage, deviation from the nonclassical bonding observed in the polyhedral boranes to a more classical organic structure might be expected; however, all of the intracage distances and angles are in the normal ranges observed in metallacarborane clusters. That all five cage carbon atoms are on the open face is again consistent with the carbon atoms favoring lower coordinate vertices,[13c] and indeed, no further carbon skeletal rearrangements for **3c** were observed even upon heating a sample to 240 °C *in vacuo*. Consistent with their bonding interactions with the iron atom, the distances between the three carbon atoms, C7, C8, and C12, are somewhat shortened (C7−C8 1.441(4) Å and C7−C12 1.423(4) Å) compared to those between the non-metal-coordinated C8, C9, and C10 carbon atoms (C9−C10 1.525(4) Å and C9−C8 1.543(4) Å). The iron atom occupies a six-coordinate position bound to three carbon atoms and three boron atoms. Again, five of the ring atoms form a plane with the C7 carbon atom distorted out of this plane 0.35 Å toward the iron atom. As a consequence, the Fe−C7 distance (1.989(2) Å) is shortened relative to Fe−C8 (2.135(3) Å) and Fe−C12 (2.106(3) Å), as well as compared to the Fe−B1, −B3, and −B6 distances. The cyclopentadienyl ring and the C8−B3−B1−B6−C12 plane are nearly parallel (dihedral angle 3.1°), with the iron atom sandwiched between the two planes (1.69 and 1.40 Å, respectively).

Although the mechanism for formation of **3c** is not yet known, it is clear from a comparison of the compositions and structures of the starting *arachno*-6-(MeC(O)CH_2)-5,6,7-$C_3B_7H_{11}^-$ anion and **3c** that the carbon atoms of the ketone side chain of the anion become incorporated into the final cage structure of **3c**. When the reaction was monitored by ^{11}B NMR, it was found that the *arachno*-6-(MeC(O)CH_2)-5,6,7-$C_3B_7H_{11}^-$ anion readily converts to the *nido*-6-(MeC(O)CH_2)-5,6,9-$C_3B_7H_9^-$ anion. Subsequent reaction of the ketone oxygen with a boron atom on the open face of the cage of this anion, followed by cyclization of the carbon framework in the manner shown in Figure 9, could, in fact, generate the structure observed for **3c** in a straightforward fashion. Such a process may be metal-

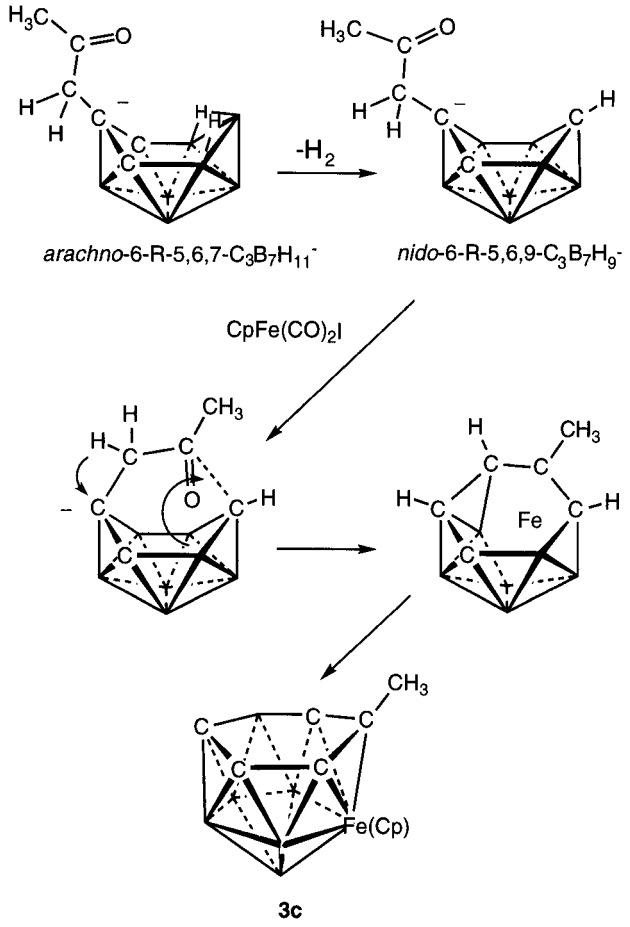

Figure 9. Possible reaction sequence leading to the formation of *nido*-2-(η-C_5H_5)Fe-7-Me-7,8,9,10,12-$C_5B_6H_{10}$, **3c**.

promoted, since control reactions carried out in the absence of $CpFe(CO)_2I$ showed no evidence of pentacarbon cage products.

Reaction of Na[Cp] with $CoCl_2$ and *arachno*-6-(NCCH$_2$)-5,6,7-$C_3B_7H_{11}^-$. The addition of Na[Cp] and K[*arachno*-6-(NCCH$_2$)-5,6,7-$C_3B_7H_{11}$] to $CoCl_2$ gave five cobaltacarborane products.

$$\mathrm{Na[C_5H_5]} + \mathrm{CoCl_2} + \mathrm{K[}\textit{arachno}\text{-6-(NCCH}_2\text{)-5,6,7-C}_3\mathrm{B}_7\mathrm{H}_{11}\mathrm{]} \xrightarrow{-\mathrm{NaCl},\ -\mathrm{KCl},\ -\mathrm{H_2}}$$

$$\textit{closo}\text{-2-}(\eta\text{-C}_5\mathrm{H}_5)\mathrm{Co\text{-}1,6\text{-}C_2B_7H_9} + \quad \textbf{4a}$$

$$\textit{closo}\text{-1-}(\eta\text{-C}_5\mathrm{H}_5)\mathrm{Co\text{-}(NCCH_2)C_3B_7H_9} + \quad \textbf{4b−d}$$

$$\textit{commo-Co}\text{-[}\textit{closo}\text{-1-Co-8,9-((}\eta\text{-C}_5\mathrm{H}_5\mathrm{)Co)_2\text{-}2,3,5\text{-}C_3B_7H_{10}]\text{-}[}\textit{closo}\text{-2′-Co-3′-(NCCH}_2\mathrm{CH_2)\text{-}1′,10′\text{-}C_2B_7H_8]} \quad \textbf{4e}$$

(7)

Compound **4a** proved to be the known compound *closo*-2-(η-C_5H_5)Co-1,6-$C_2B_7H_9$, as determined both by a comparison of its spectral data with those previously reported[8] and by a single-crystal X-ray determination (see the Supporting Information for details). Compounds **4b−d** are paramagnetic; therefore, NMR techniques could not be used for structural elucidation. However, their 1-(η-C_5H_5)Co(NCCH$_2$)$C_3B_7H_9$ compositions were confirmed by exact mass measurements and all three compounds show strong C≡N absorptions in their IR spectra, indicating that the side chain was neither cleaved nor incorporated into the cage. Although the cobaltatricarbadecaboranyl

(19) Wong, K.-S.; Bowser, J. R.; Pipal, J. R.; Grimes, R. N. *J. Am. Chem. Soc.* **1978**, *100*, 5045−5051.
(20) Maynard, R. B.; Sinn, E.; Grimes, R. N. *Inorg. Chem.* **1981**, *20*, 1201−1206.

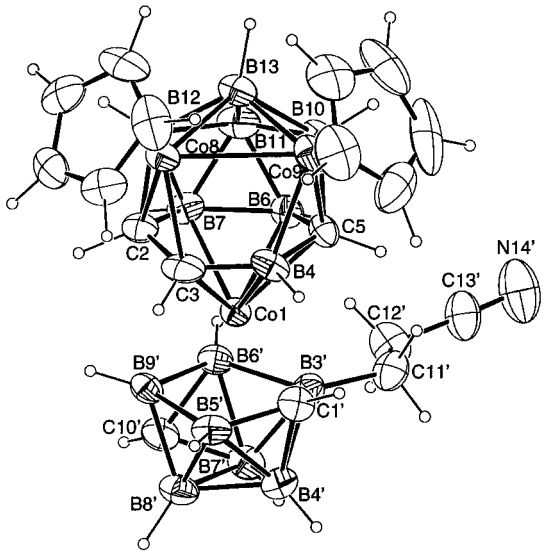

Figure 10. ORTEP diagram of the molecular structure of **4e**, *commo*-*Co*-[*closo*-1-Co-8,9-((η-C_5H_5)Co)$_2$-2,3,5-$C_3B_7H_{10}$][*closo*-2′-Co-3′-(NCCH$_2$-CH$_2$)-1′,10′-$C_2B_7H_8$].

fragments in these compounds have 25 skeletal electrons, the previous structural study[4a] of 1-(η-C_5H_5)Co-2-Me-2,3,4-$C_3B_7H_9$ has shown these types of clusters have gross octadecahedral structures similar to those of the 24-skeletal-electron closo-iron compounds discussed above, with the exception of an elongated Co−C4 distance. The exact assignment of the cage-carbon and substituent positions in **4b**−**d** cannot be conclusively made; however, their observed isomerization reactions suggest that they have structures that are analogous to **1d**, **1b,** and **1c**, respectively. Thus, as was the case for the conversion of **1c** to **1b**, the quantitative conversion of **4d** to **4c** was observed at 207 °C after 1 h, suggesting that these complexes are **4d**, 1-(η-C_5H_5)-Co-2-(NCCH$_2$)-2,3,4-$C_3B_7H_9$, and **4c**, 1-(η-C_5H_5)Co-4-(NCCH$_2$)-2,3,4-$C_3B_7H_9$, with the observed isomerization being the rearrangement of the side chain from the C2 to the C4 position. As was the case for **1d**, no isomerization of **4b** was observed, leading to its tentative assignment as the 1-(η-C_5H_5)Co-3-(NCCH$_2$)-2,3,4-$C_3B_7H_9$ isomer**.** Heating at higher temperatures (294 °C for 1 h) resulted in decomposition of all complexes.

The structure of multimetal multicage complex **4e**, *commo*-*Co*-[*closo*-1-Co-8,9-((η-C_5H_5)Co)$_2$-2,3,5-$C_3B_7H_{10}$][*closo*-2′-Co-3′-(NCCH$_2$CH$_2$)-1′,10′-$C_2B_7H_8$], was established by a single-crystal X-ray determination, as shown in the ORTEP drawing in Figure 10. The two-cage complex can be seen to be composed of a 13-vertex cluster containing three cobalt, three carbon, and seven boron atoms with one of the cobalt atoms shared, commo fashion, with a second 10-vertex cage containing two carbon and seven boron atoms. On the basis of skeletal-electron-counting rules,[13] the 13-vertex tricobalt fragment should have 28 skeletal electrons and adopt a cage structure based on a closo-docosahedron.[21] A regular docosahedron has one four-coordinate, ten five-coordinate, and two nonadjacent six-coordinate vertices. Structural studies of other 13-vertex metallacaboranes having closo structures, including *closo*-1-(η-C_5H_5)Co-7,9-$C_2B_{10}H_{12}$,[22] [*commo*-*Ti*-(Ti-1,6-Me$_2$$C_2B_{10}H_{10}$)]$^{2-}$,[23] *closo*-4-dppe-4-Pd-1,6-$C_2B_{10}H_{12}$,[24] *closo*-4,4,4-H(PPh$_3$)$_2$-2-OMe-4-Ir-1,6-$C_2B_{10}H_{11}$,[24] *closo*-1,1-(PPh$_3$)$_2$-1-H-1,2,4-RhC$_2$B$_{10}$H$_{12}$,[25] *closo*-1-Me-4-Et$_3$P-$\mu_{4,6}$-Co(PEt$_3$)$_2$-μ-(H)$_2$-4,1,2-$CoC_2B_{10}H_{10}$[26] and many tungstadicarbaborane complexes,[27] have shown that the metal atoms favor a six-coordinate position but also that there are significant skeletal distortions in these cages. These distortions occur because the atom occupying the second six-coordinate vertex in the docosahedron usually exhibits long distances to one or two of its neighboring atoms, thereby resulting in structures containing one or two quadrilateral faces, rather than the normal trigonal faces found in the polyhedral boranes. Although **4e** appears to be the first trimetal closo 13-vertex cluster, it exhibits structural features related to those of the monometal complexes. Thus, in **4e**, Co1 lies in a six-coordinate cage position bound to the C2, C3, B4, C5, B6, B7 ring. This ring is nonplanar, with both the C2 (0.26 Å) and C5 atoms (0.16 Å) distorted away from Co1 out of the plane of the remaining four atoms. The other two cobalts, Co8 and Co9, have long Co8−B4 and Co9−C3 bond lengths, 2.66(1) and 3.01(1) Å, respectively, but normal lengths to five other atoms [Co8−C3, −C2, −B12, −B13, −Co9 (Co8−ring centroid 1.36 Å) and Co9−B4, −C5, −B10, −B13, −Co8 (Co9−ring centroid 1.41 Å)]. The joining of the six-membered belt to the five-membered belt containing the Co8, Co9, B12, B11, and B10 atoms then results in the formation of a single four-membered face containing the Co8, Co9, C3, and B4 atoms between the belts. The Co8−Co9 bond distance of 2.559(2) Å is somewhat longer than the typical 2.38−2.50 Å range generally found for Co−Co bonds in cobaltacarboranes and cobaltaboranes,[28] perhaps reflecting the unusual bonding environment.

Consistent with its 22 skeletal electrons, the 10-vertex CoC_2B_7 fragment has a gross closo-bicapped square antiprismatic geometry in which the two carbon atoms are located in the two four-coordinate capping positions. The cage structure is thus similar to those proposed for the well-known *closo*-2-(η-C_5H_5)-Co-1,10-$C_2B_7H_9$ and *commo*-*Co*-(2-Co-1,10-$C_2B_7H_9$)$_2$ complexes[8] and to that which has been crystallographically established for the 2,1,10-$CoC_2B_7H_9$ fragment in the triple-decker compound (η-C_5H_5)Co(μ-η^5-Et$_4$MeC$_3$B$_2$)Co-1,10-$C_2B_7H_9$.[29] Although the carbon atom locations are different, the gross geometry is also similar to that of **4a**, *closo*-2-(η-C_5H_5)Co-1,6-$C_2B_7H_9$ (vide infra; Supporting Information). The most remarkable feature of this fragment is that it contains only *two* cage carbons. The third carbon originally present in the tricarbadecaboranyl cage has been expelled from the cluster and is now found as a component of the side chain (i.e., −CH_2CH_2CN) that is attached at the B3′ position. Thus, this side chain is now one carbon longer than that in the original anion. The resulting dicarbanonaborane fragment is, as in the monometal complexes discussed above, then functioning as a formal $RC_2B_7H_8^{2-}$ ligand toward Co1, thereby allowing Co1 to attain

(21) Brown, L. D.; Lipscomb, W. N. *Inorg. Chem.* **1977**, *12*, 2989−2996.
(22) (a) Churchill, M. R.; DeBoer, B. G. *Inorg. Chem.* **1974**, *13*, 1411−1418. (b) Churchill, M. R.; DeBoer, B. G. *Chem. Commun.* **1972**, 1326−1327.
(23) Lo, F. Y.; Strouse, C. E.; Callahan, K. P.; Knobler, C. B.; Hawthorne, M. F. *J. Am. Chem. Soc.* **1975**, *97*, 428−429.
(24) Alcock, N. W.; Taylor, J. G.; Wallbridge, M. G. H. *J. Chem. Soc., Dalton Trans.* **1987**, 1805−1811.
(25) Hewes, J. D.; Knobler, C. B.; Hawthorne, M. F. *Chem. Commun.* **1981**, 206−207.
(26) Barker, G. K.; Garcia, M. P.; Green, M.; Stone, F. G. A.; Welch, A. J. *Chem. Commun.* **1983**, 137−139.
(27) (a) Crennell, S. J.; Devore, D. D.; Henderson, S. J. B.; Howard, J. A. K.; Stone, F. G. A. *J. Chem. Soc., Dalton Trans.* **1989**, 1363−1374. (b) Brew, S. A.; Carr, N.; Mortimer, M. D.; Stone, F. G. A. *J. Chem. Soc., Dalton Trans.* **1991**, 811−822. (c) Carr, N.; Fernandez, J. R.; Stone, F. G. A. *Organometallics* **1991**, *10*, 2718−2725. (d) Carr, N.; Mullica, D. F.; Sappenfield, E. L.; Stone, F. G. A. *Organometallics* **1993**, *12*, 1131−1139.
(28) For numerous examples of Co−Co lengths in cobaltacarbaboranes and cobaltaboranes, see: Grimes, R. N. In *Comprehensive Organometallic Chemistry;* Wilkinson, G., Stone, F. G. A., Abel, E. W., Eds.; Pergamon: New York, 1982; Vol. 1, Chapter 5.5, Tables 1 and 2, pp 533−536.
(29) Weinmann, W.; Metzner, F.; Pritzkow, H.; Siebert, W.; Sneddon, L. G. *Chem. Ber.* **1996**, *129*, 213−217.

a +3 oxidation state (the 13-vertex cage is functioning as a −1 ligand toward Co1). Thus, the expulsion of the cage carbon from the smaller cage may well be driven by the need of Co1 to attain a favorable oxidation state.

In summary, the results discussed above illustrate that because of the ready loss of H_2 and carbon skeletal rearrangments, the coordination chemistry of the *arachno*-tricarbaboranes, *arachno*-6-R-5,6,7-$C_3B_7H_{12}$, is in many ways similar to that of the *nido*-6-Me-5,6,9-$C_3B_7H_{10}$ tricarbaborane. However, reactions with the *arachno*-6-R-5,6,7-$C_3B_7H_{11}^-$ anions can be used to give metallatricarbadecaboranyl complexes containing reactive side chains [$NCCH_2-$, $MeC(O)CH_2-$, $MeOC(O)CH_2-$]. Incorporation of side chain units can also occur either intermolecularly to give multicomplexes, such as ($\mu_{2,12'}$-CH_2)[*closo*-1-(η-C_5H_5)-Fe-2,3,4-$C_3B_7H_9$][*arachno*-5′-($NCCH_2$)-5′,7′,9′,12′,11′-$C_4NB_7H_{10}$], **1e**, or intramolecularly to yield, for example, the pentacarbaborane complex *nido*-2-(η-C_5H_5)Fe-7-Me-7,8,9,10,-12-$C_5B_6H_{10}$, **3c**. These results, along with the recent syntheses of a range of other higher-carbon carboranes, including tetracarbon[30] and other tricarbon[14,31−33] carboranes and their derived metallacarborane complexes, also demonstrate that a continuum of carboranes with increasing carbon compositions should be achievable and that such clusters will exhibit a diverse coordination chemistry.

Acknowledgment. We thank the National Science Foundation for support of this work.

Supporting Information Available: Tables listing infrared data, atomic positional parameters, thermal parameters, and bond distances and angles for **1c**, **1d**, **1e**, **2b**, **2c**, **3c**, **4a**, and **4e** and an ORTEP diagram of **4a** (42 pages). Ordering information is given on any current masthead page.

IC961253P

(30) (a) Grimes, R. N. *Adv. Inorg. Chem. Radiochem.* **1983**, *26*, 55−115 and references therein. (b) Grimes, R. N. *Acc. Chem. Res.* **1978**, 420−427 and references therein.

(31) (a) Štíbr, B.; Holub, J.; Teixidor, F.; Viñas, C. *Chem. Commun.* **1995**, 795−796. (b) Štíbr, B.; Holub, J.; Císarová, I.; Teixidor, F.; Viñas, C.; Fusek, J.; Plzák, Z. *Inorg. Chem.* **1996**, *35*, 3635−3642.

(32) Shedlow, A. M.; Carroll, P. J.; Sneddon, L. G. *Organometallics* **1995**, *14*, 4046−4047.

(33) See, for example: (a) Kuhlman, T.; Pritzkow, H.; Zenneck, U.; Siebert, W. *Angew. Chem., Int. Ed. Engl.* **1984**, *23*, 965−966. (b) Zwecker, J.; Pritzkow, H.; Zenneck, U.; Siebert, W. *Angew. Chem., Int. Ed. Engl.* **1986**, *25*, 1099−1100. (c) Zwecker, J.; Kuhlman, T.; Pritzkow, H.; Siebert, W.; Zenneck, U. *Organometallics* **1988**, *7*, 2316−2324. (d) Siebert, W.; Hettrich, R.; Pritzkow, H. *Angew. Chem., Int. Ed. Engl.* **1994**, *33*, 203−204. (e) Fessenbecker, A.; Hergel, A.; Hettrich, R.; Schäfer, V.; Siebert, W. *Chem. Ber.* **1993**, *126*, 2205−2210.